

Michalis Mazonakis  
Konstantin Pagonidis  
Thomas Schlosser  
Peter Hunold  
John Damilakis  
Jörg Barkhausen  
Nicholas Gourtsoyiannis

## Stereological estimation of left-ventricular volumetric and functional parameters from multidetector-row computed tomography data

Received: 3 August 2007  
Revised: 11 February 2008  
Accepted: 13 February 2008  
Published online: 20 March 2008  
© European Society of Radiology 2008

M. Mazonakis (✉) · J. Damilakis  
Department of Medical Physics,  
University Hospital of Iraklion,  
P.O. Box 1352, 71110 Iraklion,  
Crete, Greece  
e-mail: mazonak@med.uoc.gr  
Tel.: +30-2810-392342  
Fax: +30-2810-542095

T. Schlosser · P. Hunold · J. Barkhausen  
Department of Diagnostic and  
Interventional Radiology and  
Neuroradiology,  
University Hospital of Essen,  
Hufelandstrasse 55,  
45122 Essen, Germany

K. Pagonidis · N. Gourtsoyiannis  
Department of Radiology, University  
Hospital of Iraklion,  
71110 Iraklion,  
Crete, Greece

**Abstract** This study aims to optimize the stereological method for estimating left-ventricular (LV) parameters from retrospectively electrocardiography-gated 16-row MDCT and to compare stereological estimations with those by MRI. MDCT was performed in 17 consecutive patients with known or suspected coronary disease. Stereological measurements based on point counting were optimized by determining the appropriate distance between grid points. LV parameters were evaluated by standard CT analysis using a semi-automatic segmentation method. Two independent observers evaluated the reproducibility of the stereological method. End-diastolic volume (EDV) and end-systolic volume (ESV) estimations with a coefficient of error below 5% were obtained in a mean time of  $2.3 \pm 0.5$  min with a point spacing of 25 and 15 pixels, respectively. The intra- and interobserver

variability for estimating LV parameters was 2.6–4.4 and 4.9–8.2%, respectively. MRI estimations were highly correlated with those by standard CT analysis ( $R > 0.82$ ) and stereology ( $R > 0.84$ ). Stereological method significantly overestimated EDV and ESV compared to MRI (EDV:  $P = 0.0011$ ; ESV:  $P = 0.0013$ ), whereas for stroke volume (SV) and ejection fraction (EF), no difference was observed ( $P > 0.05$ ). For standard CT analysis and MRI, significant differences were found except for SV and EF (EDV:  $P = 0.0008$ ; ESV:  $P = 0.0004$ ; EF:  $P = 0.051$ ; SV:  $P = 0.064$ ). The time-efficient optimized stereological method enables the reproducible evaluation of LV function from MDCT.

**Keywords** Multidetector CT · MRI · Left ventricular volume · Left ventricular function · Stereology

### Introduction

Cardiac magnetic resonance imaging (MRI) provides high temporal and reasonable spatial resolution, while images can be acquired in any anatomic orientation. Quantitative measurements of left-ventricular (LV) volumetric and functional parameters are accurate and reproducible, making cine MRI the standard of reference [1–3]. Thin-section multidetector-row computed tomography (MDCT) of the heart, providing an excellent longitudinal spatial resolution, is increasingly employed for the reliable diagnosis of obstructive coronary artery disease and

coronary bypass grafts [4–7]. Image reformation can be performed in any desired plane. Retrospective electrocardiography (ECG) gating allows the image reconstruction in any phase of the cardiac cycle and subsequent LV volume measurements at end-diastolic and end-systolic phases [8].

Several methods have been employed for the determination of end-diastolic volume (EDV) and end-systolic volume (ESV) from MDCT short-axis reformations. The method of planimetry based on the manual tracing of endocardial contours on diastolic and systolic image series has been used [8–10]. Planimetric measurements are labor intensive and time consuming [9]. Most of the studies

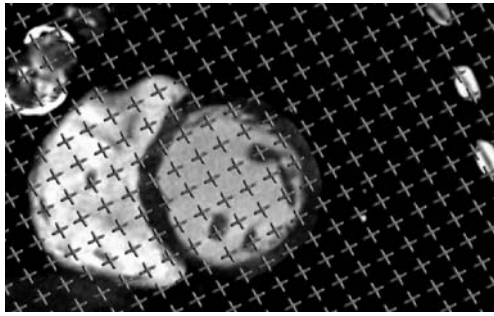


**Fig. 1** A square grid of test points is placed on a short-axis MDCT image for the stereological estimation of end-diastolic volume (EDV). The point spacing is equal to 25 pixels

dealing with cardiac function assessment have used semi-automatic segmentation techniques that are available in commercial software [11–18]. The obtained contours should be checked visually and manual adjustments to the true endocardial borders are often required [13].

To our knowledge, no reported experience exists about the stereological estimation of LV volumes using CT scans. Stereological volume measurements are based on the simple procedure of point counting and manual or semi-automatic segmentation of endocardial contours is not required. The stereological method has been successfully employed to provide efficient volume estimations of infarct and brain compartments [19], intracranial cavity [20, 21], intravertebral disc [22], liver [23], lung [24], and urinary bladder [25] from CT scans. Cardiac function has been evaluated by applying the stereological method on MR images [26, 27]. However, Roberts et al. [26] presented MR-based volume measurements of only one patient, whereas Graves and Dommert [27] made no attempts to optimize the volumetric method. The optimization procedure of the stereological method is a prerequisite whenever rapid and reliable volume assessments are needed [20, 28–30].

**Table 1** Mean values ( $\pm$ SD) of the coefficient of error (CE) and the number of counted points associated with the stereological estimation of end-diastolic volume (EDV) and end-systolic volume (ESV) from MDCT data sets using six different distances between test points of the grid

Point spacing (pixels)	EDV		ESV	
	CE (%)	No. of points	CE (%)	No. of points
10	3.8 $\pm$ 0.9	819 $\pm$ 251	4.8 $\pm$ 0.9	391 $\pm$ 185
15	3.9 $\pm$ 1.0	370 $\pm$ 112	4.9 $\pm$ 0.9	174 $\pm$ 88
20	4.3 $\pm$ 1.0	206 $\pm$ 60	5.5 $\pm$ 0.9	102 $\pm$ 48
25	4.6 $\pm$ 1.1	133 $\pm$ 41	6.4 $\pm$ 1.4	66 $\pm$ 34
30	5.2 $\pm$ 1.1	92 $\pm$ 28	7.3 $\pm$ 1.5	49 $\pm$ 23
35	5.7 $\pm$ 1.0	68 $\pm$ 21	8.4 $\pm$ 1.9	36 $\pm$ 17

**Table 2** Intraobserver and interobserver coefficient of variation (CV) values associated with the stereological estimation of left-ventricular volumetric and functional parameters from MDCT data sets

Parameter	CV (%)	
	Intraobserver	Interobserver
EDV	2.6	4.9
ESV	3.5	7.4
SV	4.4	8.2
EF	2.8	6.5

EDV End-diastolic volume, ESV end-systolic volume, SV stroke volume, EF ejection fraction

The aims of the current study were (1) to optimize the stereological method for estimating EDV, ESV, stroke volume (SV), and ejection fraction (EF) from retrospectively ECG-gated MDCT data sets, and (2) to compare these stereological estimations with the reference values obtained by cine MRI.

## Materials and methods

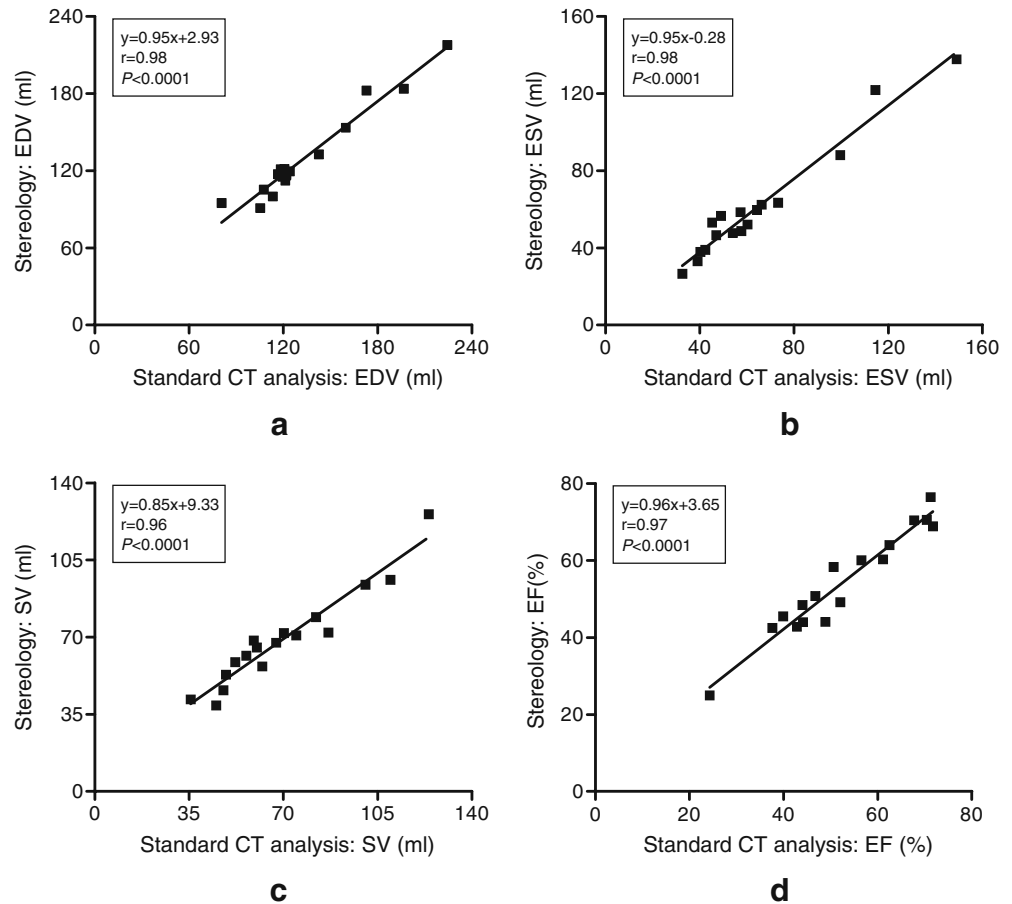
### Patients

Seventeen consecutive patients with a mean age of 58.2 $\pm$ 8.8 years were prospectively enrolled in the current study. These patients with established or suspected coronary artery disease were referred for MDCT coronary angiography. An additional cine MRI study for the assessment of LV function was performed within 12 h following CT scanning. The institutional review board approved the study protocol. All patients gave written informed consent prior to imaging examinations.

### MDCT examinations

All examinations were performed on a 16-detector-row MDCT scanner (Somatom Sensation 16, Siemens Medical Solutions, Forchheim, Germany). Scanning parameters were as follows: 420 ms gantry rotation time, 120 kV, 500 mAs, 0.75 mm beam collimation, and 3.5 mm table feed per rotation [31]. Images were acquired in the craniocaudal direction during inspiratory breath-hold while the patient's ECG trace was recorded simultaneously. Iodinated contrast agent (120 ml; 300 mg I/ml; Xenetix, Guerbet, Aulnay, France) at a flow rate of 3.5 ml/s was administered via an 18-G access into the antecubital vein. Before MDCT examination, beta-blockers (Brevibloc, Baxter, Unterschleissheim, Germany) were injected intravenously in patients with heart rates exceeding 65 beats/min at a dosage of 0.5 mg/kg.

**Fig. 2** Linear regression analysis of **a** end-diastolic volume (EDV), **b** end-systolic volume (ESV), **c** stroke volume (SV), and **d** ejection fraction (EF) estimations obtained by the stereological method and standard CT analysis



ECG-gated image reconstruction was performed in 5% steps through the entire RR interval. Twenty axial image series with a section thickness of 1.0 mm and a reconstruction increment of 0.5 mm were obtained. End-diastolic and end-systolic phases were determined as the axial images presenting the maximum and minimum cross-sectional LV areas, respectively. The axial diastolic and systolic image series were transferred to a workstation equipped with the Wizard software package (Siemens, Forchheim, Germany). Contiguous 8-mm multiplanar reformations in the short-axis orientation encompassing the entire LV from base to apex were calculated from the axial images. The pixel size in the short-axis images was  $0.45 \times 0.45 \text{ mm}^2$ . For the determination of LV volumetric and functional parameters from MDCT data, the most basal section to be included for analysis was defined as the image presenting LV myocardium in at least 50% of its perimeter. The most apical section was the image with a discernible LV lumen. Papillary muscles were included in the LV cavity.

#### Stereological estimations from MDCT data sets

In accordance with the Cavalieri principle, the volume of an object can be estimated by cutting it into equally spaced

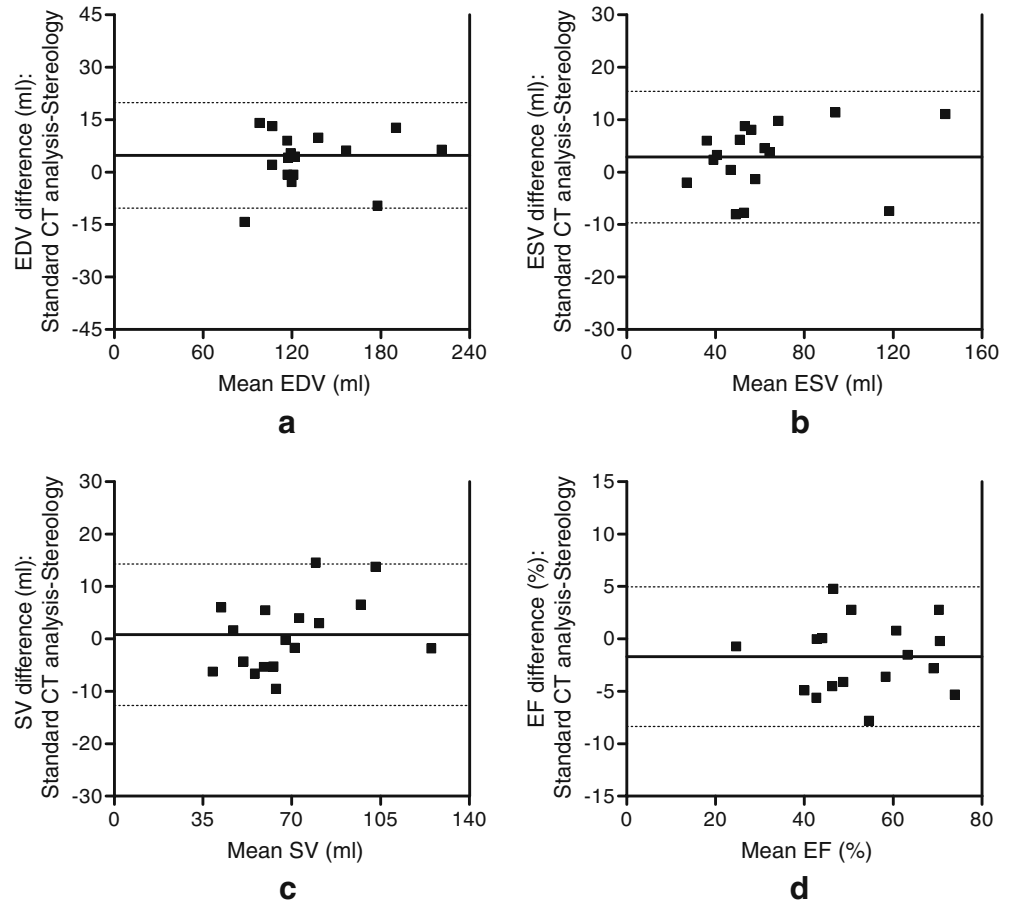
sections from end to end and measuring the area of the object on each section [32]. The estimate of the volume is given by the formula:

$$V = T \sum_{i=1}^m A_i$$

where  $T$  is the section thickness,  $m$  is the number of sections and  $A_i$  is the object area of a section  $i$ . The area is usually measured by means of the planimetric technique where the user manually delineates the borders of the object of interest on a section-by-section basis and the software program counts the voxels encompassed by the generated contours. A more efficient method for such area measurements is the stereological method of point counting [32].

Stereological measurements were carried out using the Analyze software (Mayo Foundation, Rochester, MN, USA). According to stereological method, a computer-generated square grid containing an array of test points was superimposed on the first end-diastolic image depicting the LV (Fig. 1). The orientation of the grid was randomly selected in the first short-axis image and it remained unchanged in all subsequent diastolic images. The user had to select all points falling inside the LV. To perform this

**Fig. 3** Bland-Altman scatter plots showing the difference in **a** end-diastolic volume (EDV), **b** end-systolic volume (ESV), **c** stroke volume (SV), and **d** ejection fraction (EF) estimations obtained by standard CT analysis and the stereological method against the mean value of each parameter. The *solid* and *dotted lines* denote the mean difference and 95% limits of agreement, respectively



procedure, the “passive pick” option was enabled. In the passive collection mode, the left mouse button was clicked once and then movement of the cursor over a grid point automatically caused it to be collected. The button did not have to be held down during the entire volume measurement. The procedure would stop any time after a second button click. The total number of selected points was automatically counted by the Analyze software. The above procedure was repeated for estimating the ESV.

The software provided LV volume calculations using the following formula:

$$V = TA_p \sum_{i=1}^m P_i$$

where  $A_p$  is the test point area and  $P_i$  is the number of points counted on a section  $i$ . The test point area in the square grid is given by the formula:

$$A_p = (u \times u)S$$

where  $u$  is the distance between the test points in pixels and  $S$  is the pixel area. The SV and EF were calculated by the following equations:

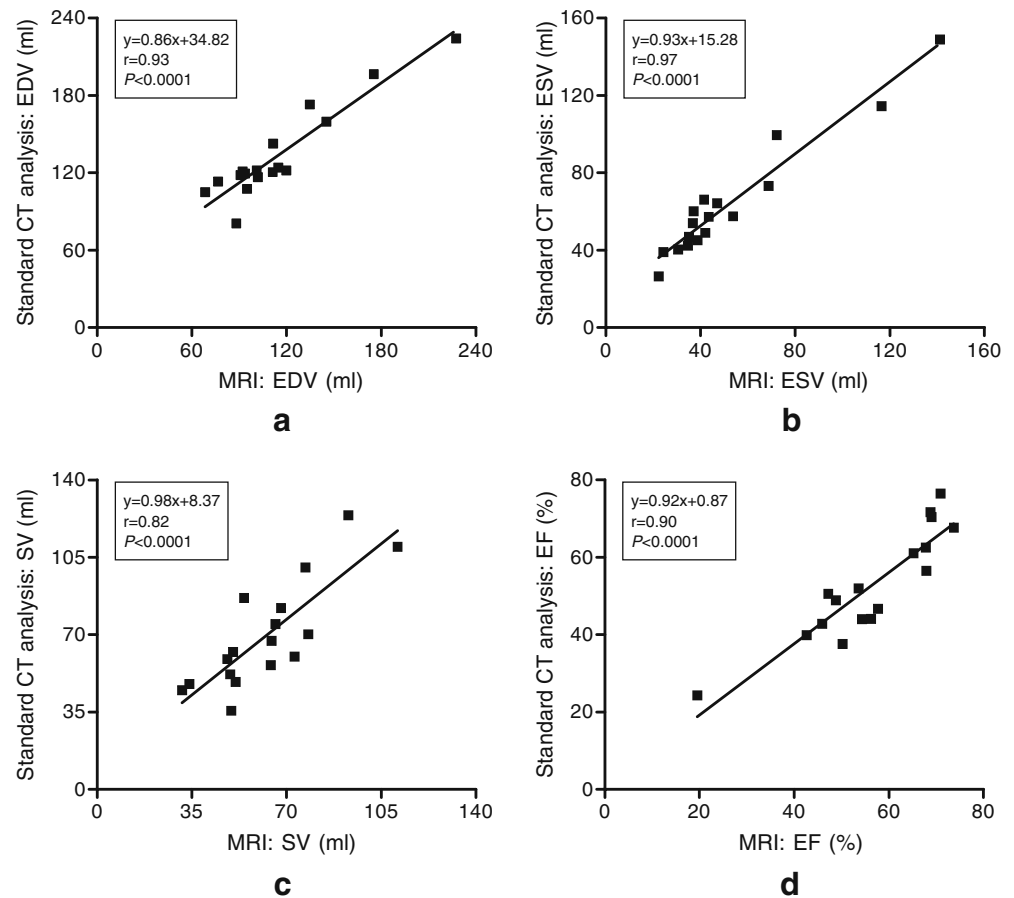
$$SV = EDV - ESV$$

$$EF = \frac{SV}{EDV} \times 100\%$$

The precision of the estimated EDV and ESV was expressed as coefficient of error (CE), which contains contributions due to both sectioning and point counting. The CE was calculated using the formula suggested by Cruz-Orive [33]:

$$CE = \left( \sum_{i=1}^m P_i \right)^{-1} \left[ \frac{1}{12} \left( 3 \sum_{i=1}^m P_i^2 + \sum_{i=1}^{m-2} P_i P_{i+2} - 4 \sum_{i=1}^{m-1} P_i P_{i+1} \right) + 0.0543 \frac{B}{\sqrt{A}} \left( m \sum_{i=1}^m P_i \right)^{0.5} \right]^{0.5}$$

**Fig. 4** Linear regression analysis of **a** end-diastolic volume (EDV), **b** end-systolic volume (ESV), **c** stroke volume (SV), and **d** ejection fraction (EF) estimations obtained by standard CT analysis and MRI



where  $B$  is the mean boundary length and  $A$  is the mean LV area. For all study participants, the quantity  $A$  was determined using the point counting process, whereas  $B$  was found by the number of intersections between the LV and a square grid of test lines [24]. The mean value of  $\frac{B}{\sqrt{A}}$ , known as the shape coefficient, was equal to 4.7. The above mean value was used for all CE calculations. Reported experience has suggested that a precision of 5% or less can be considered as sufficient in stereological applications [32]. The CE of SV and EF estimations was calculated using error propagation analysis.

#### Optimization of the stereological method

The appropriate point spacing of the test grid and the optimum sampling intensity of short-axis images for the stereological estimation of EDV and ESV were defined. The LV volumes of all patients were measured for six different distances between the test points of the grid. The following point-separation distances were used: 10, 15, 20, 25, 30, and 35 pixels. Moreover, the EDV and ESV were estimated for the sample types of 1/2 and 1/3. A sample type of 1/2 means that two samples can be systematically drawn from the total

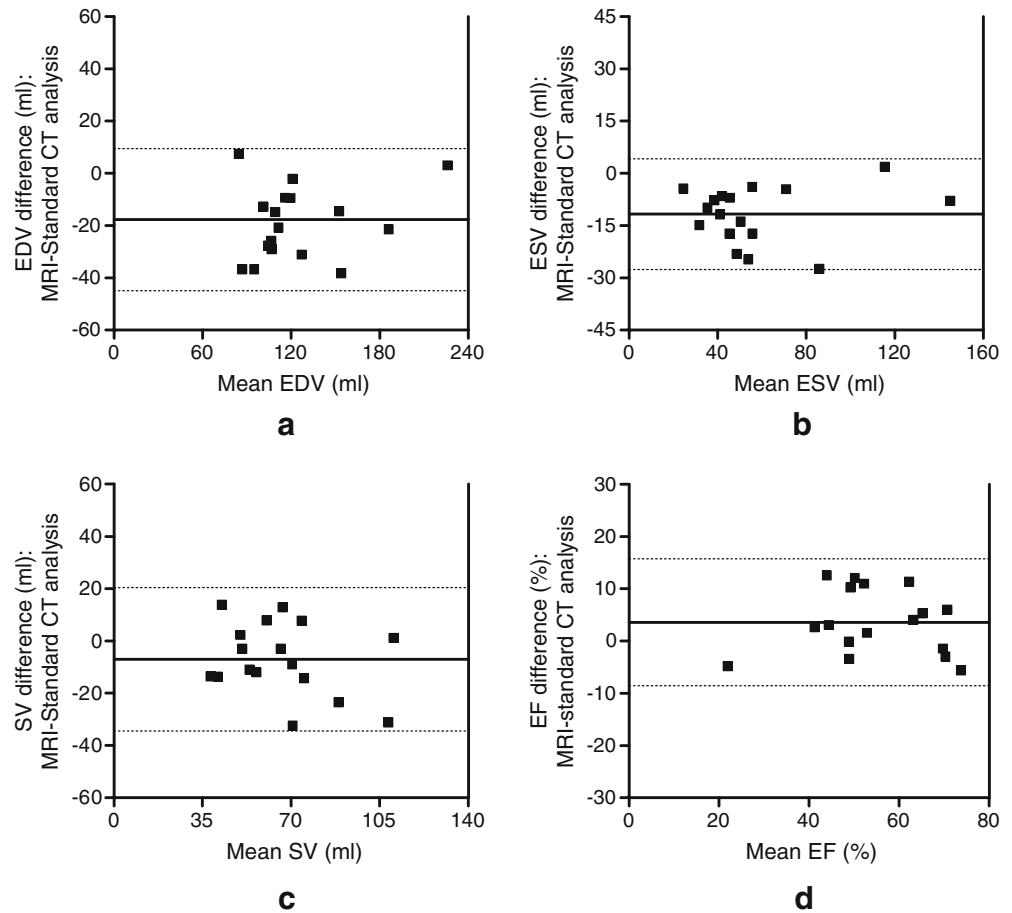
number of short-axis images depicting the LV during the end-diastolic or end-systolic phases. For example, assume an LV cavity of a patient depicted in ten end-diastolic images numbered 1,2,...,9,10. A sample type of 1/2 will yield two samples with size five. These samples will contain the images numbered {1, 3, 5, 7, 9} and {2, 4, 6, 8, 10}. Systematic sampling of MDCT image reformations was performed for the first seven patients participating in this study.

The reproducibility of the optimized stereological method was evaluated. The EDV, ESV, SV, and EF of all patients were estimated one more time by the same observer. The interval between the first and the second set of measurements was at least 25 days. To find the interobserver variability, a second independent observer experienced in both MDCT imaging and stereological applications determined the LV volumes and EF. The second observer was blinded to the results of all prior experiments. Reproducibility measurements of EDV and ESV were performed using the optimum point-spacing settings.

#### Standard CT analysis

Left ventricular volumetric and functional parameters were obtained by standard CT analysis employed in everyday

**Fig. 5** Bland-Altman scatter plots showing the difference in **a** end-diastolic volume (EDV), **b** end-systolic volume (ESV), **c** stroke volume (SV), and **d** ejection fraction (EF) estimations obtained by MRI and standard CT analysis against the mean value of each parameter. The *solid* and *dotted* lines denote the mean difference and 95% limits of agreement, respectively



clinical practice. The analysis was performed using a commercially available software (Argus, Siemens, Forchheim, Germany). The software supports the semi-automatic detection of endocardial contours in diastolic and systolic MDCT images with a discernible LV cavity. All the segmented contours were studied visually and the LV borders were manually corrected using software tools if necessary. The software provided calculations of all parameters.

**Table 3** Mean values ( $\pm$ SD) and range of the left-ventricular volumetric and functional parameters estimated by the stereological method and cine MRI

Parameter	Stereology		MRI	
	Mean $\pm$ SD	Range	Mean $\pm$ SD	Range
EDV (ml)	129.6 $\pm$ 34.9	91.1–217.9	114.6 $\pm$ 39.0	68.5–227.4
ESV (ml)	60.9 $\pm$ 29.5	28.0–137.9	52.1 $\pm$ 32.0	22.3–141.2
SV (ml)	68.7 $\pm$ 21.6	39.0–125.8	62.5 $\pm$ 20.2	31.4–111.0
EF (%)	53.9 $\pm$ 13.0	25.0–72.0	56.4 $\pm$ 13.7	19.5–73.7

EDV End-diastolic volume, ESV end-systolic volume, SV stroke volume, EF ejection fraction

## MRI study

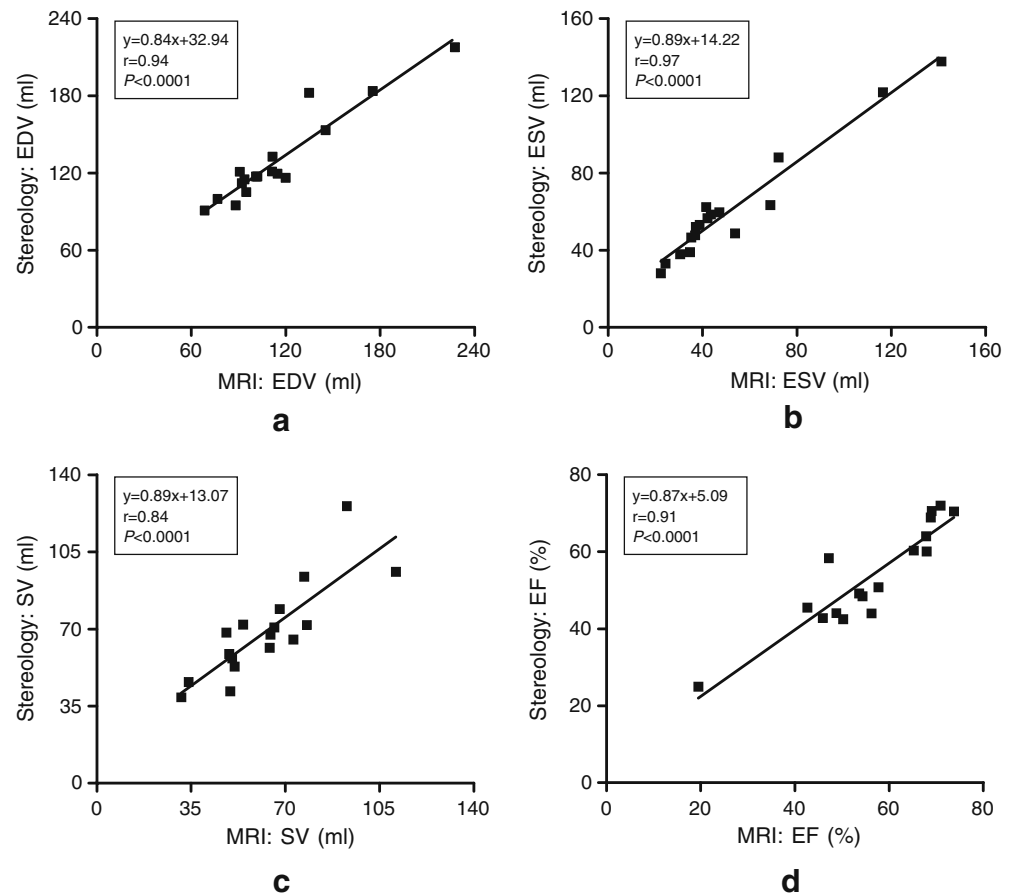
MRI studies were generated on a 1.5-Tesla whole-body scanner (Magnetom Sonata, Siemens, Erlangen, Germany). The phased-array torso coil and the table-integrated spine coil were employed for signal reception. All patients were examined in supine position during inspiratory breath-hold. A prospectively ECG-gated steady-state free precession cine sequence (TR/TE: 3.0/1.5, flip angle: 60°) was acquired in the short-axis orientation. The entire heart was encompassed with 8-mm sections with no interslice gap. An independent observer with experience in cardiac MRI analyzed short-axis images using the Argus software (Siemens, Forchheim, Germany). The papillary muscles were regarded as being part of the LV cavity. The most basal section to be included for analysis had to cover more than 50% of the LV circumference.

## Statistical analysis

Stereological estimations were compared with those by standard CT analysis. Moreover, LV volumetric and functional parameters estimated by cine MRI were



**Fig. 6** Linear regression analysis of **a** end-diastolic volume (EDV), **b** end-systolic volume (ESV), **c** stroke volume (SV), and **d** ejection fraction (EF) estimations obtained by the stereological method and MRI



compared with the respective values determined by MDCT using the stereological method or standard analysis. Linear regression analysis was performed to examine the relation between different modalities or different volumetric CT methods. A Wilcoxon matched-pairs test was employed to detect possible statistical differences. The Bland-Altman statistical method was used to illustrate the limits of agreement [34]. For each LV parameter, the difference between the values obtained by MDCT and MRI or by the two methods applied on MDCT short-axis reformations was plotted against their mean. Based on the Bland-Altman analysis, the 95% limits of agreement were defined as the mean difference  $\pm 1.96SD$ , where SD is the standard deviation of the differences.

For the optimized stereological method, the SD of measurements obtained by stereological and MRI estimations was plotted against the mean of measurements in order to examine whether the agreement depends upon the size of the volumetric or functional parameter. Intra- and interobserver variability in the stereological estimation of EDV, ESV, SV, and EF was expressed as coefficient of variation (CV) values. A *P*-value of less

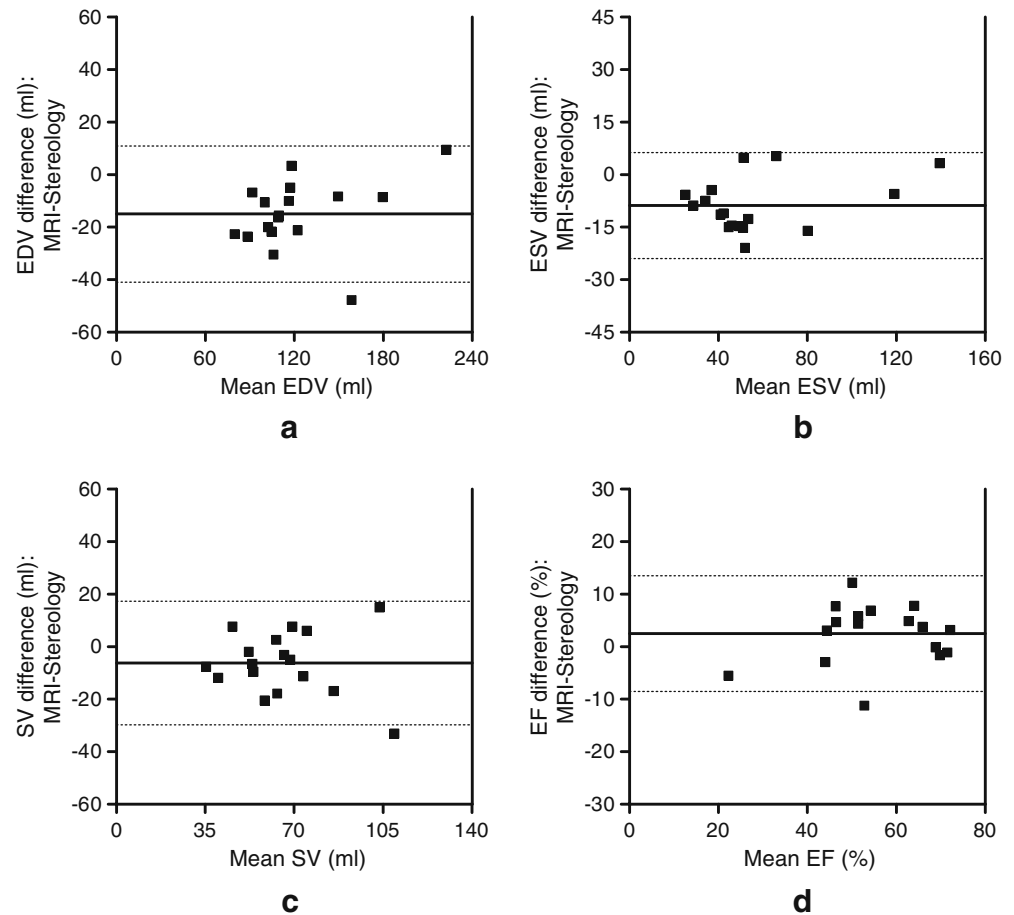
than 0.05 was considered to indicate statistical significance. All statistical analyses were performed using the software GraphPad Prism version 4.0 (GraphPad Software, CA, USA).

## Results

### Optimization of stereological method

The mean CE and the mean number of counted points for the six different distances between the test points of the grid that were employed during stereological EDV and ESV estimations are given in Table 1. The increase in point spacing resulted in a considerable reduction in the number of counted points and, therefore, in a reduction of the time required. The mean time needed to estimate EDV with a point spacing of 10, 15, 20, 25, 30, and 35 pixels was equal to 3.7, 2.2, 1.6, 1.2, 1.1, and 0.9 min, respectively. The corresponding times for ESV estimation were 2.0, 1.1, 1.0, 0.9, 0.9, and 0.8 min, respectively. Based on the results of Table 1, all point distances of 25 pixels or smaller provided

**Fig. 7** Bland-Altman scatter plots showing the difference in **a** end-diastolic volume (EDV), **b** end-systolic volume (ESV), **c** stroke volume (SV), and **d** ejection fraction (EF) estimations obtained by MRI and the stereological method against the mean value of each parameter. The *solid* and *dotted* lines denote the mean difference and 95% limits of agreement, respectively



acceptable EDV estimations with a CE of less than 5%. The point spacing of 25 pixels was considered as the optimum one because it could provide volume estimates with acceptable levels of precision, while simultaneously reducing the time measurement in comparison with that required for point distances of 10, 15, and 20 pixels. For the same reasons, we decided that the optimum point spacing for ESV estimation is equal to 15 pixels. Stereological EDV and ESV measurements with the aforementioned optimum point-spacing settings were performed in a total mean time of  $2.3 \pm 0.5$  min with a range of 1.8–2.9 min. All above volume estimations were obtained by applying the stereological method on the total number of end-diastolic or end-systolic images depicting the LV cavity. For all point separation distances, the CEs of EDV estimations arising from a sample type of 1/2 and 1/3 were more than 5.6 and 8.9%, respectively. The corresponding CEs for ESV estimation exceeded 7.6 and 10.8%, respectively.

The mean CEs of the obtained SV and EF estimations were  $6.6 \pm 1.0$  and  $5.6 \pm 1.5\%$ , respectively. The intra- and

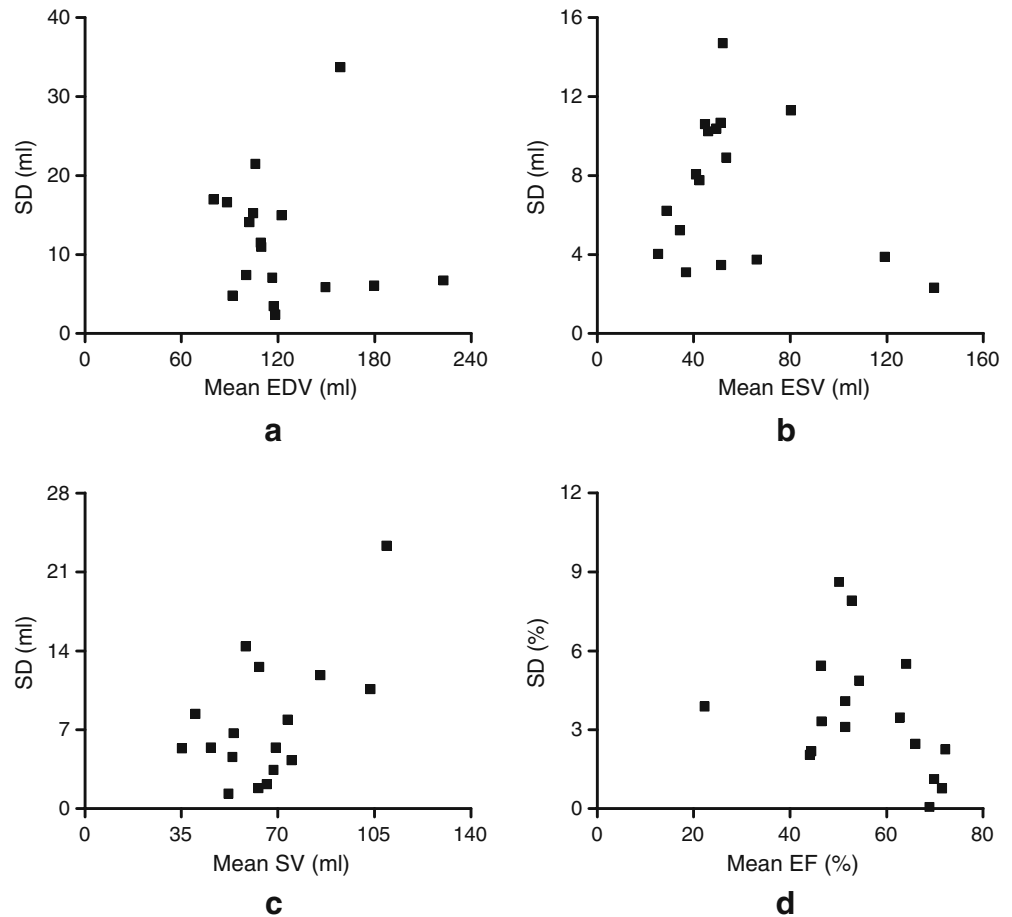
interobserver CV values associated with the stereological measurement of all LV volumetric and functional parameters from MDCT data sets are presented in Table 2.

#### Comparison of stereological method with standard CT analysis

An excellent correlation was found between the stereological method and standard CT analysis based on the semi-automatic tracing of endocardial borders (Fig. 2). The spread of the differences between the two methods is presented in Fig. 3. The mean difference between EDV, ESV, SV, and EF values derived by standard CT analysis and the stereological method was  $4.8 \pm 7.7$  ml,  $2.9 \pm 6.4$  ml,  $0.8 \pm 6.9$  ml, and  $-1.7 \pm 3.4\%$ , respectively. There was no statistical difference between the two methods (EDV:  $P=0.057$ ; ESV:  $P=0.071$ ; EF:  $P=0.061$ ; SV:  $P=0.878$ ). The mean duration for EDV and ESV measurements as performed by an experienced radiologist in standard CT analysis was  $4.2 \pm 1.2$  min.



**Fig. 8** Plots showing the standard deviation (SD) of **a** end-diastolic volume (EDV), **b** end-systolic volume (ESV), **c** stroke volume (SV), and **d** ejection fraction (EF) estimations obtained by the stereological method and MRI against the mean value of each parameter



#### Comparison of standard CT analysis with MRI

Left-ventricular volumetric and functional parameters obtained by standard CT analysis correlated well with the respective MRI estimations (Fig. 4). Bland-Altman statistical method for EDV, ESV, SV, and EF displayed a mean difference of  $-17.7 \pm 13.9$  ml,  $-11.7 \pm 8.1$  ml,  $-7.0 \pm 14.0$  ml, and  $3.6 \pm 6.2\%$ , respectively (Fig. 5). Statistically significant differences were found for EDV and ESV (EDV:  $P=0.0008$ ; ESV:  $P=0.0004$ ). EF and SV estimations obtained by standard analysis of MDCT short-axis reformations and MRI did not differ significantly (EF:  $P=0.051$ ; SV:  $P=0.064$ ).

#### Comparison of stereological and MRI estimations

Stereological estimations of all volumetric and functional parameters from MDCT data sets and MRI-based measurements are summarized in Table 3. An excellent correlation was found between stereological and MRI estimations (Fig. 6). The Bland-Altman scatter plots are shown in Fig. 7. For each plot, no more than one data point was outside the 95% limits of agreement. Based on Bland-

Altman analysis, the mean difference between MRI and the stereological method for estimating EDV, ESV, SV, and EF was  $-15.0 \pm 13.2$  ml,  $-8.8 \pm 7.7$  ml,  $-6.2 \pm 12.0$  ml, and  $2.5 \pm 5.6\%$ , respectively. For each parameter, the SD of stereological and MRI estimations versus the mean of these estimations is presented in Fig. 8. No significant correlation was found except for SV (EDV:  $R=-0.09$ ,  $P=0.73$ ; ESV:  $R=-0.25$ ,  $P=0.33$ ; EF:  $R=-0.36$ ,  $P=0.15$ ; SV:  $R=0.56$ ,  $P=0.02$ ), where  $R$  is the correlation coefficient. The Wilcoxon test showed that stereological estimations on short-axis image reformations significantly overestimated the LV volumes (EDV:  $P=0.0011$ ; ESV:  $P=0.0013$ ). For EF and SV, there was no statistically significant difference between the stereological method and MRI (EF:  $P=0.067$ ; SV:  $P=0.064$ ).

#### Discussion

In the current study, the stereological method was used to determine the LV volumetric and functional parameters from MDCT data sets. The stereological method can be optimized either by altering the point spacing of the square test grid or by systematically sampling short-axis images. The CE of the LV volumes derived by the systematical

sampling procedure exceeded the target precision of 5%. To obtain an acceptable level of precision, stereological volume estimations should be carried out on all images depicting the LV cavity during the end-diastolic and end-systolic phases. Analytical measurements revealed that the optimum point spacing for EDV and ESV estimation is 25 and 15 pixels, respectively. These separation distances between test points of the grid can be employed in all stereological measurements irrespective of the LV size. This may be attributed to the population of this study including consecutive patients with a wide variation in cardiac volumes. The use of optimum point spacing results in quick and acceptable LV volume estimations with a CE below 5%.

The optimized stereological method was found to be reproducible, as reflected by the relatively small intra- and interobserver variability values. The interobserver variability for the stereological estimation of all volumetric and functional parameters was similar to the values of previous studies that performed manual or semi-automatic segmentation of endocardial contours on MDCT image reformations. They reported that the interobserver variability for the measurement of EDV, ESV, SV, and EF was 2.0–7.2, 4.0–9.5, 3.0–9.0, and 2.0–8.7%, respectively [10, 14, 35–38]. To our knowledge, only one study of Sugeng et al. [37] evaluated the intraobserver variability in EDV, ESV, and EF measurements from MDCT data. Their CV values of 2.0–2.2% are comparable with those presented here.

Statistical analysis revealed that the stereological method and standard CT approach based on the semi-automatic segmentation of endocardial contours in diastolic and systolic images are in good agreement. Both volumetric methods applied on MDCT short-axis reformations overestimated EDV and ESV in comparison with the reference standard cine MRI. Several previous studies have concluded that LV volume measurements from MDCT agree well with MRI [13, 17, 35, 38]. Van der Vleuten et al. [39] reported that MDCT volume measurements are interchangeable with those obtained by MRI. However, other studies have reported similar findings to ours [10, 31, 37, 40]. The overestimation of the LV volume during the end-systolic phase should be attributed to the limited temporal resolution of MDCT. The 16-MDCT system used in the current study provides a temporal resolution of approximately 210 ms whereas that of MRI is reduced to 40 ms. A temporal resolution of 30–50 ms is necessary to define the peak systolic constriction and depict the minimum systolic LV volume [3]. The limited temporal

resolution of MDCT can not lead to increased EDV values compared with MRI. The significant EDV overestimation might be due to intermodality differences related to the depiction of LV in a series of short-axis images. Regarding the SV and EF, the differences between stereological and MRI estimations were found to be not statistically significant. Therefore, the minor underestimation of EF and overestimation of SV by the stereological method should not be considered as clinically important.

The proposed method for LV volumetric and functional analysis from MDCT data sets has several limitations. One limitation is patient exposure to ionizing radiation during CT. Sixteen-slice MDCT coronary angiography on the same scanner with that employed in our study results in a patient effective dose range from 9 to 13 mSv [15, 17, 18]. The use of ECG controlled tube current modulation can considerably reduce the above radiation doses [41]. Moreover, a relatively small number of consecutive patients were examined, and the majority of them presented a normal LV function. The optimized stereological measurements, as described here, can not provide information about the ventricular mass. Further research is required to adapt the stereological method and MDCT data for LV mass determination.

The efficiency of stereological volumetric estimations on short-axis reformations is strongly affected by the temporal resolution of the 16-detector-row MDCT scanner employed. Recent technological developments in CT systems resulting in reduced gantry rotation times down to 330 ms may considerably improve the temporal resolution. Flohr et al. [42] reported that dual-source CT provides a temporal resolution as low as 83 ms, independent of the patient's heart rate. The new generation of MDCT systems permitting the simultaneous acquisition of 64 submillimeter slices can yield a temporal resolution of 42–165 ms [43]. However, the better temporal resolution of 64-MDCT scanners is associated with a higher patient dose than that observed during 16-slice cardiac angiography [41, 44, 45].

In conclusion, the optimized stereological method allows the quick determination of EDV and ESV from MDCT short-axis reformations. The good agreement of stereological SV and EF estimations with the respective cine MRI calculations gives strong evidence about the accuracy of the above parameters. The analysis of LV function based on stereological volume estimations obtained from MDCT data sets is reproducible.

## References

1. Alfakih K, Reid S, Jones T, Sivananthan M (2004) Assessment of ventricular function and mass by cardiac magnetic resonance imaging. *Eur Radiol* 14:1813–1822
2. Barkhausen J, Ruehm SG, Goyen M, Buck T, Laub G, Debatin JF (2000) MR evaluation of ventricular function: true fast imaging with steady-state precession versus fast low-angle shot cine MR imaging—feasibility study. *Radiology* 219:264–269
3. Setser RM, Fischer SE, Lorenz CH (2000) Quantification of left ventricular function with magnetic resonance images acquired in real time. *J Magn Reson Imaging* 12:430–438

4. Nieman K, Cademartiri F, Lemos PA, Raaijmakers R, Pattynama PM, de Feyter PJ (2002) Reliable noninvasive coronary angiography with fast submillimeter multislice spiral computed tomography. *Circulation* 106:2051–2054
5. Kuetner A, Beck T, Drosch T, Kettering K, Heuschmid M, Burgstahler C, Claussen CD, Kopp AF, Schroeder S (2005) Diagnostic accuracy of non-invasive coronary imaging using 16-detector slice spiral computed tomography with 188 ms temporal resolution. *J Am Coll Cardiol* 45:123–127
6. Schlosser T, Konorza T, Hunold P, Kühl H, Schmermund A, Barkhausen J (2004) Noninvasive visualization of coronary artery bypass grafts using 16-detector row computed tomography. *J Am Coll Cardiol* 44:1224–1229
7. Vanhoenacker PK, Heijenbrok-Kal MH, Van Heste R, Decramer I, Van Hoe LR, Wijns W, Hunink MG (2007) Diagnostic performance of multidetector CT angiography for assessment of coronary artery disease: meta-analysis. *Radiology* 244:419–428
8. Juergens KU, Fischbach R (2006) Left ventricular function studied with MDCT. *Eur Radiol* 16:342–357
9. Boehm T, Alkadhri H, Roffi M, Willmann JK, Desbiolles LM, Marincek B, Wildermuth S (2004) Time-effectiveness, observer dependence, and accuracy of measurements of left ventricular ejection fraction using 4-channel MDCT. *Rofo* 176:529–537
10. Grude M, Juergens KU, Wichter T, Paul M, Fallenberg EM, Muller JG, Heindel W, Breithardt G, Fischbach R (2003) Evaluation of global left ventricular myocardial function with electrocardiogram-gated multidetector computed tomography. Comparison with magnetic resonance imaging. *Invest Radiol* 38:653–661
11. Dewey M, Müller M, Teige F, Hamm B (2006) Evaluation of a semiautomatic software tool for left ventricular function analysis with 16-slice computed tomography. *Eur Radiol* 16:25–31
12. Dewey M, Müller M, Eddicks S, Schnapauff D, Teige F, Rutsch W, Borges AC, Hamm B (2006) Evaluation of global and regional left ventricular function with 16-slice computed tomography, biplane cineventriculography, and two-dimensional transthoracic echocardiography. Comparison with magnetic resonance imaging. *J Am Coll Cardiol* 48:2034–2044
13. Juergens KU, Grude M, Maintz D, Fallenberg EM, Wichter T, Heindel W, Fischbach R (2004) Multi-detector row CT of left ventricular function with dedicated analysis software versus MR imaging: initial experience. *Radiology* 230:403–410
14. Juergens KU, Seifarth H, Maintz D, Grude M, Ozgun M, Wichter T, Heindel W, Fischbach R (2006) MDCT determination of volume and function of the left ventricle: are short-axis image reformations necessary? *Am J Roentgenol* 186:S371–S378
15. Fischbach R, Juergens KU, Ozgun M, Maintz D, Grude M, Seifarth H, Heindel W, Wichter T (2007) Assessment of regional left-ventricular function with multidetector-row computed tomography versus magnetic resonance imaging. *Eur Radiol* 17:1009–1017
16. Koch K, Oellig F, Oberholzer K, Bender P, Kunz P, Mildnerberger P, Hake U, Kreitner K, Thelen M (2005) Assessment of right ventricular function by 16-detector-row CT: comparison with magnetic resonance imaging. *Eur Radiol* 15:312–318
17. Mahnken AH, Koos R, Katoh M, Spuentrup E, Busch P, Wildberger JE, Kühl HP, Günther RW (2005) Sixteen-slice spiral CT versus MR imaging for the assessment of left ventricular function in acute myocardial infarction. *Eur Radiol* 15:714–720
18. Montaudon M, Laffon E, Berger P, Corneloup O, Latrabe V, Laurent F (2006) Measurement of cardiac ventricular volumes using multidetector row computed tomography: comparison of two- and three-dimensional methods. *Eur Radiol* 16:2341–2349
19. Lyden PD, Zweifler R, Mahdavi Z, Lonzo L (1994) A rapid, reliable, and valid method for measuring infarct and brain compartment volumes from computed tomographic scans. *Stroke* 25:2421–2428
20. Mazonakis M, Karampekios S, Damilakis J, Voloudaki A, Gourtsoyiannis N (2004) Stereological estimation of total intracranial volume on CT images. *Eur Radiol* 14:1285–1290
21. Sahin B, Acer N, Sonmez OF, Emizreoglu M, Basaloglu H, Uzun A, Bilgic S (2007) Comparison of four methods for the estimation of intracranial volume: a gold standard study. *Clin Anat* 20:766–773
22. Bilgic S, Sahin B, Sonmez OF, Odaci E, Colakoglu S, Kaplan S, Ergur H (2005) A new approach for the estimation of intravertebral disc volume using the Cavalieri principle and computed tomography images. *Clin Neurol Neurosurg* 107:282–288
23. Emizreoglu M, Sahin B, Selcuk MB, Kaplan S (2005) The effects of section thickness on the estimation of liver volume by the Cavalieri principle using computed tomography images. *Eur J Radiol* 56:391–397
24. Pache JC, Roberts N, Vock P, Zimmermann A, Cruz-Orive LM (1993) Vertical LM sectioning and parallel CT scanning designs for stereology: application to human lung. *J Microsc* 170:9–24
25. Mazonakis M, Damilakis J, Varveris H (1998) Bladder and rectum volume estimations using CT and stereology. *Comp Med Imag Graph* 22:195–201
26. Roberts N, Cruz-Orive LM, Bourne M, Herfkens RJ, Karwoski RA, Whitehouse GH (1997) Analysis of cardiac function by MRI and stereology. *J Microsc* 187:31–42
27. Graves MJ, Dommert DMF (2000) Comparison of cardiac stroke volume measurement determined using stereological analysis of breath-hold cine MRI and phase contrast velocity mapping. *Br J Radiol* 73:825–832
28. Cotter D, Miszkiel K, Al-Sarraj S, Wilkinson ID, Paley M, Harrison MJG, Hall-Griggs MA, Everall IP (1999) The assessment of postmortem brain volume; a comparison of stereological and planimetric methodologies. *Neuroradiology* 41:493–496
29. Mazonakis M, Damilakis J, Maris T, Prassopoulos P, Gourtsoyiannis N (2002) Comparison of two volumetric techniques for estimating liver volume using magnetic resonance imaging. *J Magn Reson Imaging* 15:557–563
30. Mazonakis M, Damilakis J, Mantatzis M, Prassopoulos P, Maris T, Varveris H, Gourtsoyiannis N (2004) Stereology versus planimetry to estimate the volume of malignant liver lesions on MR imaging. *Magn Reson Imaging* 22:1011–1016
31. Schlosser T, Pagonidis K, Herborn CU, Hunold P, Waltering KU, Lauenstein TC, Barkhausen J (2005) Assessment of left ventricular parameters using 16-MDCT and new software for endocardial and epicardial border delineation. *Am J Roentgenol* 184:765–773
32. Gundersen HJG, Jensen EB (1987) The efficiency of systematic sampling in stereology and its prediction. *J Microsc* 147:229–263

33. Cruz-Orive LM (1993) Systematic sampling in stereology. *Bull Int Stat Inst* 55:451–468
34. Bland JM, Altman DG (1986) Statistical methods for assessing agreement between two methods of clinical measurement. *Lancet* I:307–310
35. Belge B, Coche E, Pasquet A, Vanoverschelde J, Gerber BL (2006) Accurate estimation of global and regional cardiac function by retrospectively gated multidetector row computed tomography. Comparison with cine magnetic resonance imaging. *Eur Radiol* 16:1424–1433
36. Halliburton SS, Petersilka M, Schwartzman PR, Obuchowski N, White RD (2003) Evaluation of left ventricular dysfunction using multiphase reconstructions of coronary multi-slice computed tomography data in patients with chronic ischemic heart disease: validation against cine magnetic resonance imaging. *Int J Cardiovasc Imaging* 19:73–83
37. Sugeng L, Mor-Avi V, Weinert L, Niel J, Ebner C, Steringer-Mascherbauer R, Schmidt F, Galuschky C, Schummers G, Lang RM, Nesser HJ (2006) Quantitative assessment of left ventricular size and function. Side-by-side comparison of real-time three-dimensional echocardiography and computed tomography with magnetic resonance reference. *Circulation* 114:654–661
38. Yamamuro M, Tadamura E, Kubo S, Toyoda H, Nishina T, Ohba M, Hosokawa R, Kimura T, Tamaki N, Komeda M, Kita T, Konishi J (2005) Cardiac functional analysis with multi-detector row CT and segmental reconstruction algorithm: comparison with echocardiography, SPECT, and MR imaging. *Radiology* 234:381–390
39. van der Vleuten PA, Willems TP, Götte MJW, Tio RA, Greuter MJW, Zijlstra F, Oudkerk M (2006) Quantification of global left ventricular function: comparison of multidetector computed tomography and magnetic resonance imaging. A meta-analysis and review of the current literature. *Acta Radiol* 47:1049–1057
40. Heuschmid M, Rothfuss JK, Schroeder S, Fenchel M, Stauder N, Burgstahler C, Franow A, Kuzo RS, Kuettner A, Miller S, Claussen CD, Kopp AF (2006) Assessment of left ventricular myocardial function using 16-slice multidetector-row computed tomography: comparison with magnetic resonance imaging and echocardiography. *Eur Radiol* 16:551–559
41. Hausleiter J, Meyer T, Hadamitzky M, Huber E, Zankl M, Martinoff S, Kastrati A, Schömig A (2006) Radiation dose estimates from cardiac multislice computed tomography in daily practice. Impact of different scanning protocols on effective dose estimates. *Circulation* 113:1305–1310
42. Flohr TG, McCollough CH, Bruder H, Petersilka M, Gruber K, Süß C, Grasruck M, Stierstorfer K, Krauss B, Raupach R, Primak AN, Küttner A, Achenbach S, Becker C, Kopp A, Ohnesorge BM (2006) First performance evaluation of a dual-source CT (DSCT) system. *Eur Radiol* 16:256–268
43. Mahnken AH, Hohl C, Suess C, Bruder H, Mühlenbruch G, Das M, Günther RW, Wildberger JE (2006) Influence of heart rate and temporal resolution on left-ventricular volumes in cardiac multislice spiral computed tomography: a phantom study. *Invest Radiol* 41:429–435
44. Dewey M, Hoffmann H, Hamm B (2007) CT coronary angiography using 16 and 64 simultaneous detector rows: intraindividual comparison. *Rofo* 179:581–586
45. Primak AN, McCollough CH, Bruesewitz MR, Zhang J, Fletcher JG (2006) Relationship between noise, dose, and pitch in cardiac multi-detector row CT. *Radiographics* 26:1785–1794